Extended Abstracts of the 2012 International Conference on Solid State Devices and Materials, Kyoto, 2012, pp1243-1244

X-Ray Three-Dimensional Topography Analysis of Basal-Plane Dislocations and Threading Edge Dislocations in 4H-SiC

Ryohei Tanuma[1], Daisuke Mori[2], Isaho Kamata[1] and Hidekazu Tsuchida[1]

[1] Central Research Institute of Electric Power Industry (CRIEPI)
2-6-1 Nagasaka, Yokosuka, Kanagawa, 240-0101 Japan
Tel: +81-070-5562-1533 E-mail: tanuma@criepi.denken.or.jp
[2] Fuji Electric Co., Ltd.
1, Fuji-machi, Hino, Tokyo, 191-8502 Japan

1. Introduction

In 4H-SiC bipolar devices, basal plane dislocations (BPDs) severely degrade the device performance due to the expansion of Shockley-type stacking faults in an epilayer [1]. One promising method to reduce BPD density in an epilayer is converting BPDs to threading-edge dislocations (TEDs) near the epilayer/substrate (E/S) interface. However, the conversion mechanism must be better understood to ensure sufficient BPD-TED conversion [2]. We have used X-ray three-dimensional (3D) topogaphy to investigate BPDs and TEDs, observing characteristic BPD-image narrowing just before the BPD-TED conversion [3]. This paper describes the morphologic and strain analyses of the BPD-TED conversion process.

2. Experimental

Figure 1 shows the setup of 3D-topography measurements. The sample examined is an 8°-off-cut (0001) Si-face 4H-SiC wafer with a 20-μm-thick epilayer. Measurements were conducted on the synchrotron beam line BL24XU at SPring-8 [4], using an X-ray microbeam with a photon energy of 15 keV. The full widths at half maximum (FWHMs) of the microbeam were typically 1.9 and 0.6 μm in horizontal and vertical directions, respectively, while the beam divergence was approximately 25 μrad in the horizontal direction, and the photon flux was about 5×10^6 photons/s on the sample. This method uses a V-slit in the microbeam X-ray diffraction for a pinpoint measurements at point Q where the incident beams crossed the extension of the V-slit transmission beam. Scanning the sample positions provides depth-resolved 3D topography [3, 5, 6].

The diffraction geometry is shown in Fig. 2. Measurements were performed with **g** = 1 1 -2 12 ($2\theta = 68.3°$) by using a Bragg-case asymmetric-reflection geometry in which the rocking angle (between the incident beam and crystal surface) was $\omega \sim 13.5°$. The beam incidence direction projected on the basal plane points the [-1 -1 2 0] direction. We use a common right-handed coordinate in Figs. 2 and 3.

Measurements were carried out in 3D-single-scan (3DSS) mode for the 3D imaging of reflection intensities and 2D-multi-scan (2DMS) mode for strain analysis. In the 3DSS mode, sample positions were scanned in three dimensions at a fixed ω value, while in the 2DMS mode, the 2D data of reflection intensities were acquired for a desired cross section at step-scanned ω values. The consecutive image data obtained in the 2DMS mode were reconstructed to rocking curves at all 2D positions, and effective misorientations (ω shifts from the average) $\Delta\omega$ were calculated by applying Gaussian fitting to each of the rocking curves [3, 6].

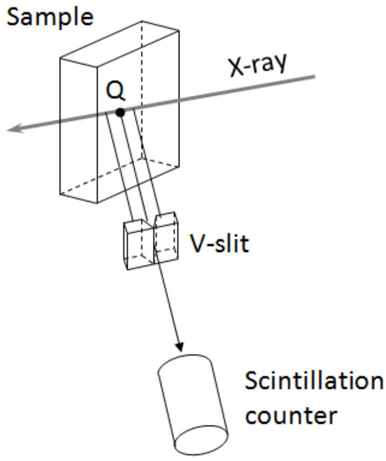

Fig. 1. Setup of microbeam X-ray diffraction for 3D topography.

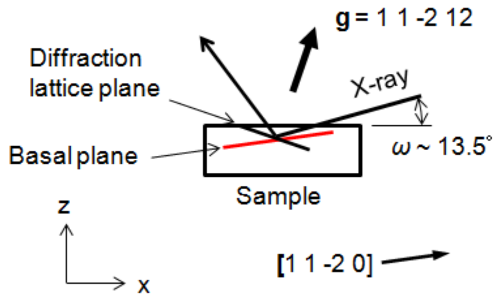

Fig. 2. Diffraction geometry

3. Results and discussion

The 3DSS measurement was performed with a cubic voxel size of 1 μm near the E/S interface, providing the stereographic isosurface images shown in Fig. 3(a). It is

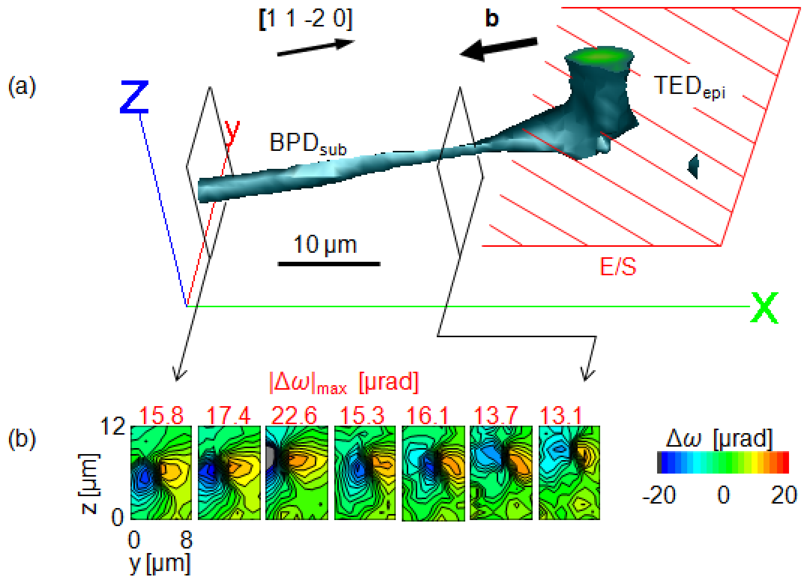

Fig. 3. Results of 3DSS (a) and 2DMS (b) measurements

clearly shown that a BPD (BPD$_{sub}$) converts into a TED (TED$_{epi}$) near the E/S interface. The TED is confirmed to have the Burgers vector **b** pointing in the [-1 -1 2 0] direction [7]. Note here that the BPD image first narrows and then changes to a thick standing TED image. This narrowing does not occur if a BPD propagates into the epilayer without the conversion. We investigated three conversion and nonconversion cases respectively, and observed BPD-image narrowing in the former, but not the latter [8].

The 2DMS measurements were also conducted, and the $\Delta\omega$ images (strain maps) typical of screw-type dislocations [6] were obtained for the y-z cross sections of BPD$_{sub}$ as shown in Fig. 3(b). In these strain maps, the positive and negative values of $\Delta\omega$ correspond to the lattice tilt in the negative and positive directions along the x-axis, respectively. We now note $|\Delta\omega|_{max} = (\Delta\omega_{max} - \Delta\omega_{min})/2$, the values of which are indicated above the strain maps [Fig. 3(b)]. It can be seen that $|\Delta\omega|_{max}$ decreases as the BPD$_{sub}$ image narrows. The 3D topography image will be dominated by kinematical direct images [3]. It is known that kinematical diffraction dominates in the mosaic region where $|\Delta\omega|$ exceeds the widths of the theoretical rocking curve [9, 10]. We hence consider that the decrease in $|\Delta\omega|_{max}$ reduces the mosaic region along the BPD; resulting in image narrowing [3]. However, the cause of the $|\Delta\omega|_{max}$ decrease remains unclear and further analysis is necessary to explain the BPD-TED conversion mechanism.

In conclusion, 3D topography analyses were conducted for the BPD-TED conversion process. The BPD image narrowing is explained by the reduction in the mosaic region along the BPD.

Acknowledgements

We would like to thank Assoc. Prof. Y. Tsusaka of the University of Hyogo for the fine tuning of the X-ray microbeam. This work was performed as part of research proposal numbers 2011A3237 and 2011B3237 of SPring-8. This research is partly supported by the Japan Society for the Promotion of Science (JSPS) through its “Funding Program for World-Leading Innovative R&D on Science and Technology (FIRST Program)".

References

[1] M. Skowronski, S. Ha: J. Appl. Phys. **99** (2006) 011101.
[2] H. Tsuchida, M. Ito, I. Kamata, M. Nagano: Phys. Status Solidi B **246** (2009) 1553.
[3] R. Tanuma, D. Mori, I. Kamata and H. Tsuchida: Appl. Phys. Express **5** (2012) 061301.
[4] S. Takeda, K. Yokoyama, Y. Tsusaka, Y. Kagoshima, J. Matsui, A. Ogura: J. Synchrotron Radiat. **13** (2006) 373.
[5] R. Tanuma, T. Kubo, F. Togoh, T. Tawara, A. Saito, K. Fukuda, K. Hayashi, Y. Tsusaka: Phys. Status Solidi A **204** (2007) 2706.
[6] R. Tanuma, T. Tamori, Y. Yonezawa, H. Yamaguchi, H. Matsuhata, K. Fukuda, K. Arai: Material Sci. Forum **615-617** (2009) 251.
[7] I. Kamata, M. Nagano, H. Tsuchida, Yi. Chen, M. Dudley: J. Cryst. Growth **311** (2009) 1416.
[8] R. Tanuma, D. Mori, I. Kamata and H. Tsuchida: Material Sci. Forum **717-720** (2012) 323.
[9] J. E. A. Miltat, D. K. Bowen: J. Appl. Cryst. **8** (1975) 657.
[10] M. Dudley, X. R. Huang, W. Huang: J. Phys. D: Appl. Phys. **32** (1999) A139.